Tekhnê
January - June 2020, Vol. 17, No. 1, pp. 25 – 36

ISSN 1692-8407

Review of strategies for input current reconstruction

Revisión de estrategias para reconstrucción de la corriente de entrada

Angélica V. Rendón C.[1] and Fredy H. Martínez S.[2]
[1]Facultad de Ingeniería, Universidad Distrital Francisco José de Caldas, Bogotá, Colombia
avrendonc@correo.udistrital.edu.co
[2]Facultad Tecnológica, Universidad Distrital Francisco José de Caldas, Bogotá, Colombia
fhmartinezs@udistrital.edu.co

Understanding the theory of active power factor correction in single-phase regulators can be quite complex for young students. This is even more critical if one considers the diversity of strategies that exist, their combinations, and even the existence of both passive and active strategies. In some way, all these approaches seek to reconstruct the input current signal, but the strategy used may be significantly different in each case. This article aims to present an overview of these techniques that can be used as a starting point for the study and design of equipment.

Keywords: Active correction, harmonic distortion, power factor, signal reconstruction, single-phase rectifiers

Entender la teoría de la corrección activa del factor de potencia en reguladores monofásicos puede ser bastante complejo para jóvenes estudiantes. Esto es aún más critico si se considera la diversidad de estrategias que existen, sus combinaciones, e incluso la existencia de estrategias tanto pasivas como activas. De alguna forma todas estas estrategias buscan reconstruir la señal de corriente de entrada, pero la estrategia utilizada puede ser sensiblemente diferente en cada caso. En este artículo se busca presentar una visión general de estas estrategias que sirva de punto de partida tanto para estudio como para el diseño de equipos.

Palabras clave: Corrección activa, distorsión armónica, factor de potencia, reconstrucción de señal, rectificadores monofásicos

---

Article typology: Research

Received: June 9, 2020
Accepted: June 26, 2020

Research funded by: Universidad Distrital Francisco José de Caldas (Colombia).

How to cite: Rendón, A., Martínez, F. (2020). *Review of strategies for input current reconstruction*. Tekhnê, 17(1), 25 -36.

ISSN 1692-8407

Introduction

The vast majority of electrical energy generated worldwide corresponds to alternating current (AC), the systems of generation, transmission, and distribution of electrical energy (power system) are designed for this form of current (Liu et al., 2016; Pahlevani et al., 2014). However, the current loads used in the different electrical energy consumption equipment require direct current (DC), largely due to the electronic component that is part of the load (Martínez, 2009b; Martínez et al., 2013). Given the large number of low and medium power devices that require a power supply, their impact on the power system is a major problem (Martínez et al., 2019). These devices obtain their direct current using a rectifier circuit, or AC-DC converter, which takes the energy from the power system and rectifies it (Akther et al., 2019). These circuits are implemented with semiconductor elements such as diodes and thyristors in controlled and uncontrolled schemes, which ensure that the electric current flows through the load always in the same direction (Martínez & Jacinto, 2013). However, with these schemes, the current drained from the power network behaves as pulses due to the conduction intervals of the rectifier circuits (Martínez, 2003). The rectifier circuits turn out to have a non-linear behavior that changes the waveform of the current signal in the power network (and of the voltage as a consequence of voltage drops), which is a major problem since this is done in an enormous amount of medium and low power equipment simultaneously. These electrical current peaks lead to a lot of problems for the power system, among which we can mention: high harmonic content in the electrical current, low efficiency of the rectifier circuit as a consequence of the high RMS value of its input current, low power factor (PF) as a consequence of the distorted current, and losses in power equipment designed to operate with low-frequency signals (Martínez & Gómez, 2004).

Due to the large amount of this equipment connected to the grid, and the cumulative consequences for the power system, several agencies have considered limits for the injection of harmonics, intending to guarantee the quality of the electrical power (Martínez, 2001). Among these standards and norms are the IEC (International Electrotechnical Commission) 61000-3-2 (electromagnetic compatibility, applied in Europe), EN 50006, VDE Standard 0160 for converters, and the ANSI/IEEE 519-1992 Standard for compensation in power converters, applied in the United States (Ochoa et al., 2017). To comply with these recommendations, numerous schemes for the reconstruction of the input current signal have been proposed in the specialized literature (Martínez & Gómez, 2012). According to how this process is performed, these correctors can be classified into passive, active, and hybrid schemes (Jauch & Biela, 2016). Passive schemes usually do not provide a complete solution to the problem and have cost and efficiency problems. On the other hand, active methods pose complexity and reliability problems, leaving hybrid schemes as the ideal configuration with the best advantages (Martínez, 2009a; Martínez & Gómez, 2007; Riaño et al., 2012; Vásquez & Martínez, 2011).

In this paper we seek to present in a summarized form, by way of documentation, the different existing schemes for power factor correction in the rectification stage of medium and low power equipment (single-phase equipment below 16 A). As stated in the literature, these schemes have been separated into three groups according to the behavior of the elements that perform the correction: passive methods, active methods, and hybrid methods. For each case, a description of the scheme, its general circuit, and its behavior as a correction scheme is presented. The structure of the rest of the document is as follows, in the next section a methodological overview is presented with the classification of the analyzed methods. The third section details each of the methods and their principle of operation. Finally, the fourth section presents our conclusions.

Methodological Overview

Given the high impact and its wide use, this discussion focuses on the correction schemes of the current signal at the input of single-phase rectifier circuits, in medium and low power applications (de Souza et al., 2019). Traditionally the problem is addressed in two ways, passively by installing filters, and actively by power converters that implement some control scheme on semiconductor devices operating at a frequency much higher than the frequency of the power network (Monteiro et al., 2019). Considering the advantages and disadvantages of each case, it is possible to include a third classification in which hybrid schemes are implemented with the support of both filters and high-frequency switched elements (Fig. 1). In any case, the objective is to return the current signal to its sinusoidal form and in phase with the voltage signal, so that the power factor returns to the nominal value of one. This is why these schemes are also known as power factor correctors (PFC) or resistive emulators.

Due to the high generation of current harmonics produced by single-phase rectifier circuits, their extended use in the power system can place the system at an operating point that exceeds international standards. Among the problems that this entails is a decrease in the quality of the power supplied, negative effects on system equipment such as harmonic losses in all equipment, reduction in installed capacity, current peaks in power capacitors, and consequently, oversizing of equipment, particularly power transformers. For reference, Tables 1 and 2 show the harmonic limits for IEC 61000-3-2 and IEEE 519-1992 standards.

ISSN 1692-8407

Figure 1

Classification of methodologies for current reconstruction according to the control scheme (Kazem, 2007).

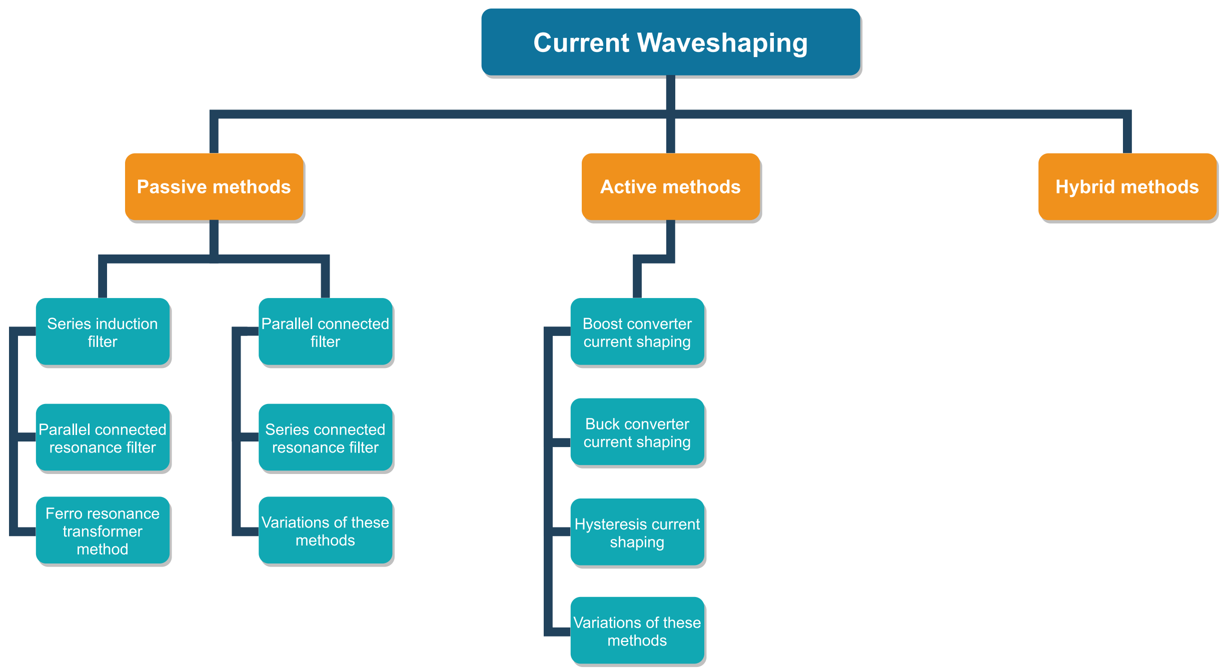

Table 1

Harmonic current limits allowed by IEC 61000-3-2 for class A equipment (balanced three-phase and single-phase equipment not included in other classes).

Harmonic order h	Maximum allowable harmonic current [A]
Odd harmonics	
3	2.30
5	1.14
7	0.77
9	0.40
11	0.33
13	0.21
$15 \leqslant h \leqslant 39$	$2.25/h$
Even harmonics	
2	1.08
4	0.43
6	0.30
$8 \leqslant h \leqslant 40$	$1.84/h$

As mentioned, the generation of electrical energy is done by transforming another energy form into electrical machines using the rotational movement of electric charge in a magnetic field. This produces electrical signals of periodical behavior, specifically of sinusoidal type. The current signal is distorted because of the non-linear loads that produce current peaks, but it is still a periodical signal. This current $i(t)$ is a non-sinusoidal periodical signal that can be analyzed by decomposing its fundamental $i_1(t)$ (component at the mains frequency, 50 Hz or 60 Hz depending on the country) and its h harmonic components $i_h(t)$ (frequencies multiplied by the fundamental). This is written as follows:

$$i(t) = i_1(t) + \sum_{h=2}^{\infty} i_h(t) \tag{1}$$

The harmonic distortion of a waveform represents the harmonic content of that signal. The amount of distortion in a voltage or current waveform is quantified by an index called total harmonic distortion (THD). This index is defined for mains voltages and currents as shown in Eqs. 2 and 3. In these equations, V_1 and I_1 correspond to the fundamental voltage and current components respectively, and V_h and I_h the h-harmonics, all in RMS terms.

$$THD_V = \frac{\sqrt{\sum_{h=2}^{\infty} V_h^2}}{V_1} \tag{2}$$

ISSN 1692-8407

Table 2

Harmonic current limits $\left(\frac{I_h}{I_1}\%\right)$ *established by IEEE 519-1992 for the non-linear load connected to the utility grid at the point of connection.* I_{SC} *is the maximum short circuit current, and* I_1 *is the maximum fundamental current. Even harmonics are limited to 25% of the limits for odd harmonics.*

I_{SC}/I_1	Order of odd harmonics h					THD [%]
	h<11	11<h<17	17<h<23	23<h<35	35<h	
< 20	4.0	2.0	1.5	0.6	0.3	5.0
20 - 50	7.0	3.5	2.5	1.0	0.5	8.0
50 - 100	10.0	4.5	4.0	1.5	0.7	12.0
100 - 1000	12.0	5.5	5.0	2.0	1.0	15.0
> 1000	15.0	7.0	6.0	2.5	1.4	20.0

$$THD_I = \frac{\sqrt{\sum_{h=2}^{\infty} I_h^2}}{I_1} \tag{3}$$

Under these conditions, the power factor (PF) is defined as the product of the displacement power factor (DPF) and the ratio $\frac{I_1}{I_S}$ (Eq. 4). In this equation, DPF corresponds to $cos\varphi$, where φ is the phase angle between voltage and current. As can be seen, the power factor is closely linked to the harmonic distortion, the higher the harmonic distortion, the higher the total current I_S concerning its fundamental component I_1 (since the rest are harmonics), so that the power factor decreases. Therefore, the presence of harmonics in the current has a very negative effect on the efficiency with which the equipment provides power to the network, and it is a very important aspect to control, not only for safety but also for effectiveness.

$$PF = \frac{P}{S} = \frac{I_1}{I_S} \times DPF \tag{4}$$

Strategies for the Reconstruction of the Current Signal

Passive methods

These methods use passive elements (inductors and capacitors) to try to improve the input current waveform and therefore provide the circuit with at most a gain of one. This strategy involves a series supply reactor that functions as a tuned harmonic filter (in series or parallel). The most common methods are the inductive filter, the resonant filter, and the ferroresonant transformer.

Series Induction Filters (SIF)

To attenuate the ripple of a rectified signal, a capacitor is commonly used in parallel with the load of the circuit. Intuitively, it can also be noted that using a series inductance

Figure 2

Full wave rectifier with inductive filter on the DC side.

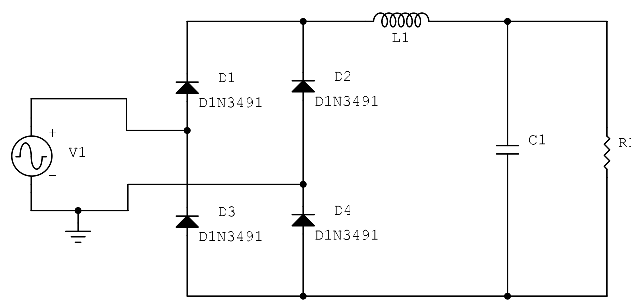

the ripple value in the load can be reduced (low-pass filter). By connecting a coil with a capacitor in an L-mount, it is possible to take advantage of each of these filters and obtain excellent results in both low and high power consumption. This inductor can be placed before (AC side) or after the bridge rectifier (DC side), then place the inductor in series with the output of the diode bridge, and analyze approximately how the output signal behaves (Fig. 2).

A full-bridge rectified signal can be expressed in the Fourier series. In the expression found there is a constant term and a series of terms of alternating characteristics at the frequency of 2ω, 4ω, 6ω,.... A coil placed in series with the load (in this case with the equivalent impedance of the capacitor in parallel with the load) behaves as a low-pass filter. In this way, the continuous signal will pass through the inductor (this being short for it), and of the time-varying signals, the 2ω frequency signal will be the least attenuated. Accordingly, in the following analysis, the other components of frequencies higher than 2ω are neglected (note that the

ISSN 1692-8407

4ω frequency harmonic is in amplitude only 20% of the amplitude of the 2ω component).

The impedances of the circuit elements are as follows based on this approximation of the signal incident on the filter:

$$\text{Capacitor} \rightarrow \frac{1}{2j\omega C} \tag{5}$$

$$\text{Inductor} \rightarrow 2j\omega L \tag{6}$$

In the circuit we have a divider formed by X_L and X_C in parallel with the load R. Depending on the incident ripple v_{ri}, the output ripple v_r will be:

$$v_r(t) = v_{ri}(t) \frac{X_L || R}{X_L + (X_C || R)} \tag{7}$$

For the capacitor to operate effectively, that is, for the capacitor to be able to supply the load, it is necessary to have to:

$$\left(X_L \middle|\middle| R\right) << R \tag{8}$$

In other words:

$$\frac{1}{2\omega C} << R \Rightarrow C >> \frac{1}{2\omega R} \tag{9}$$

And, for this case, the expression for the output ripple is:

$$v_r \approx v_{ri} \frac{X_C}{X_L + X_C} \tag{10}$$

Since a small ripple is desired, the value to be chosen for X_L must be large compared to X_C, i.e:

$$2L\omega >> \frac{1}{2\omega C} \Rightarrow L >> \frac{1}{4\omega^2 C} \tag{11}$$

Which produces a ripple of:

$$v_r \approx v_{ri} \frac{X_C}{X_L} \tag{12}$$

The ripple factor is defined as:

$$r = \frac{V_{r(eff)}}{V_{med}} \tag{13}$$

Where:

$$V_{r(eff)} = \frac{V_{r(pico)}}{\sqrt{2}} = \frac{4V_p}{3\pi\sqrt{2}} \frac{X_C}{X_L} \tag{14}$$

$$\text{and } V_{med} = \frac{2V_p}{\pi} \tag{15}$$

Therefore, the ripple factor is defined as:

$$r = \frac{\sqrt{2}}{3} \frac{X_C}{X_L} = \frac{\sqrt{2}}{3} \frac{1}{4\omega^2 LC} \tag{16}$$

At 60 Hz, and expressing the values of C in μ-Farads and L in Henries, we have that:

$$r = \frac{0.83}{LC} \tag{17}$$

The configuration shown in Fig. 2 can operate in a continuous or discontinuous mode according to the current conduction in the diode bridge. The expressions stated above are valid as long as they do not imply a current reversal in the coil (which diodes do not allow). This inversion will occur when the peak value of the ripple current $\left(\sqrt{2}I_{r(eff)}\right)$ becomes equal to the average current $\left(I_{med} = \frac{V_{med}}{R}\right)$. To avoid this current reversal, it must be kept in mind that:

$$I_{med} \geq \sqrt{2}I_{r(eff)} \tag{18}$$

Where:

$$I_{r(eff)} = \frac{V_{r(eff)}}{X_C} = \frac{rV_{med}}{X_C} = \frac{\sqrt{2}}{3} \frac{V_{med}}{X_L} \tag{19}$$

And replacing this in condition (18):

$$\frac{V_{med}}{R} \geq \frac{2}{3} \frac{V_{med}}{X_L} \Rightarrow X_L \geq \frac{2R}{3} \tag{20}$$

This is the value known as critical inductance, which defines the operating mode of the circuit. Since this analysis is approximate, in practice this value should be increased by at least 25% to ensure continuous mode operation.

At low current consumption levels, the above characteristic is not fulfilled, and the L-filter behaves as a capacitive filter (Fig. 3). Above a certain value of consumption I_0 the L-filter operates normally and the established results can be applied. It should be noted that the output resistance R_{output} for power consumption greater than I_0 is equal to the sum of the coil resistance and the rectifier resistance. The equivalent model of this type of filtering is shown in Fig. 4.

This approximation of the first harmonic tends to overestimate the continuous conduction limit and the value of the critical inductance must be corrected. Let us now observe the effect on the PF. The voltage applied to the circuit is as follows:

$$v_1(t) = V_{med} + V_{1P}\cos(2\omega t)$$

Average rectified voltage (V_{med})

Number of alternating voltages to be rectified (2)

Amplitude of the first harmonic (V_{1P})

$$v_1(t) = \frac{2V_p}{\pi} - \frac{4V_p}{3\pi}\cos(2\omega t) \tag{21}$$

ISSN 1692-8407

Figure 3

Control curve for the inductive filter.

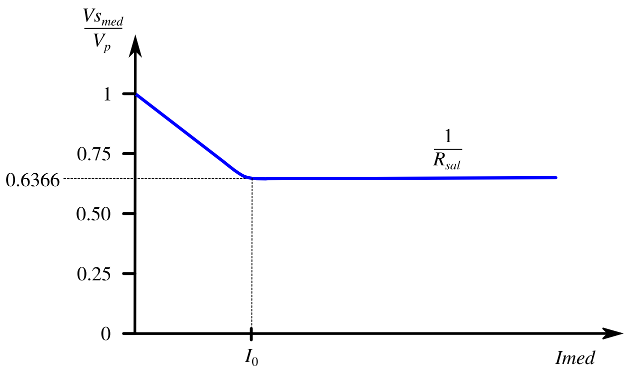

Figure 4

Equivalent model of the inductive filter on DC side.

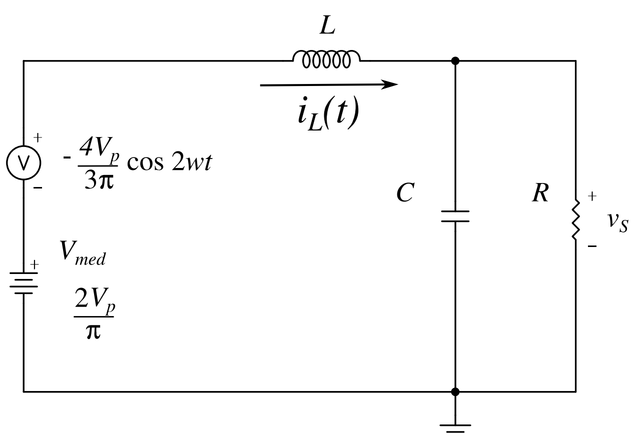

In continuous conduction we have:

$$v_1(t) = \frac{2V_p}{\pi} - \frac{4V_p}{3\pi}\cos(2\omega t) = L\frac{di_L(t)}{dt} + i_L(t)[R \parallel C] \quad (22)$$

$$v_1(t) = L\frac{di_L(t)}{dt} + i_L(t)\left[\frac{R}{1+\omega^2R^2C^2} + \frac{\omega R^2C}{j(1+\omega^2R^2C^2)}\right] \quad (23)$$

Taking:

$$R' = \frac{R}{1+\omega^2R^2C^2} \quad (24)$$

It is concluded that:

$$v_1(t) = \frac{2V_p}{\pi} - \frac{4V_p}{3\pi}\cos(2\omega t) = L\frac{di_L(t)}{dt} + R'i_L(t) + E \quad (25)$$

Where E would represent the complex part of this voltage. Solving this equation leads easily to:

$$i_L(t) = \frac{\frac{2V_p}{\pi} - E}{R'} + \frac{\frac{4V_p}{\pi}}{3\sqrt{R'^2 + L^2 4\omega^2}}\cos\left(2\omega t - \arctan\frac{2\omega L}{R'}\right) \quad (26)$$

To simplify the expressions and facilitate their analysis, the following parameter will be used:

$$K = \frac{2L}{R'T} \quad (27)$$

This parameter K is called the conduction parameter (in reality this parameter is usually indicated as a function of the load resistance R and not as a function of R', however, due to the value assigned to R', this change does not affect the results that will be reached). From this, the circuit current is:

$$i_L(t) = \frac{\frac{2V_p}{\pi} - E}{R'} + \frac{\frac{4V_p}{\pi}\cos\left(2\omega t - \arctan\frac{2\omega L}{R'}\right)}{3R'\sqrt{1+4K^2\pi^2}} \quad (28)$$

From this statement it can be deduced:

- The average value of the current:

$$I_{med} = \frac{\frac{2V_p}{\pi} - E}{R'} \quad (29)$$

- The r.m.s. value of the current:

$$I_{L(eff)} = \sqrt{\left[\frac{\frac{2V_p}{\pi} - E}{R'}\right]^2 + \left[\frac{\sqrt{2}\frac{2V_p}{\pi}}{3R'\sqrt{1+4K^2\pi^2}}\right]^2} \quad (30)$$

- The current form factor (r.m.s. current value of $i_L(t)$ referred to I_{med}):

$$FF = \frac{I_{L(eff)}}{I_{med}} = \sqrt{1 + \frac{\left[\frac{\sqrt{2}\frac{2V_p}{\pi}}{3R'\sqrt{1+4K^2\pi^2}}\right]^2}{\left[\frac{\frac{2V_p}{\pi}-E}{R'}\right]^2}} \quad (31)$$

Now, the active power at the output is equal to:

$$P = \frac{1}{T}\int_{-T/2}^{T/2} v_1(t)\, i_L(t)\, dt = \frac{1}{T}\int_{-T/2}^{T/2}\left(R'i_L(t)^2 + L\, i_L(t)\frac{di_L(t)}{dt} + E\, i_L(t)\right)dt \quad (32)$$

$$P = E\, I_{med} + R' I_{L(eff)}^2 \quad (33)$$

Where:

- $E\, I_{med}$ is the useful term corresponding to the power transformed by the load.

ISSN 1692-8407

- $R' I^2_{L(eff)}$ is the term corresponding to the Joule losses in the load and in the filter inductance connected in series with it.

For good load performance, the second term needs to be very small compared to the first term. The increase of the current form factor $i_L(t)$ (FF) causes an increase of the various apparent powers, while the active power increases little. Thus, it leads to a reduction of the overall power factor.

Most of the increase in the form factor corresponds, for a given $E \times I_{med}$ value, to an increase in the ripple currents and Joule current losses in the load, in the semiconductors, in the secondary and primary windings of the transformer, and the power supply line. To seek a low ripple in the rectified current, and therefore a high PF value, the value of the conduction parameter K must be increased.

By increasing the value of this conduction parameter the current waveform changes to the ideal case of an approximately square current waveform (Fig. 5). In this case, the PF obtained is 0.9, which is the maximum value obtainable with this type of filter.

However, this type of solution has a major problem, the size of the components used. For example, to feed a 2.1 kW inverter at 120 Vdc requires a 228 mH inductor, with a maximum stored energy of 54 Joules to obtain a PF close to 0.9. The size of the inductor is exaggerated, and therefore, so is its cost. Because of this, solution variants have been implemented to avoid these sizes and costs. One of the most commonly used variants is shown in Fig. 6 and consists of adding a capacitor to the secondary of the system power transformer (C_2) which is used to minimize the current wave distortion factor. The inductance L is then placed to minimize current harmonics in the line by decreasing the current wave displacement, and C_1 is calculated so that the rectified voltage has no significant ripple.

For analysis and testing purposes, this circuit was simulated in SPICE 3 (Simulation Program with Integrated Circuit Emphasis of the University of California, Berkeley) (Nagel & McAndrew, 2018; Sellers et al., 2018)for the following characteristics:

- Type of load: Resistive.
- Power consumed by the load in stationary state: 1920 W.
- DC voltage supplying the load: 120 V.

Using the circuit in Fig. 6, to obtain 120 V DC on the load, for the 3.3 mH inductor, an AC voltage is required at the output of the transformer secondary of:

$$V_p = 170 \text{ V} \tag{34}$$

$$V_{i(eff)} \approx 120.2 \text{ V} \tag{35}$$

And the load has a value of:

$$R = \frac{120^2}{1920} = 7.5\ \Omega \tag{36}$$

Without any type of correction, the diodes would withstand peaks of at least 10 times the nominal current (almost 200 A), so the 1N3491 diode was selected for the rectification, which considerably exceeds these margins.

After a four-cycle transient, stationary behavior of the input current is observed (Fig. 7). Although the current is no longer sinusoidal and resembles somewhat the square behavior identified above, it tries to conduct throughout the network cycle and with little deviation concerning the voltage signal.

Resonant filter

This method is a variant of the use of low-pass filters, in which tuned LC type arrays are used to reduce the amplitude of a certain harmonic, usually those that occur with greater amplitude in the circuit, i.e. third, fifth and seventh harmonic. By surgically eliminating the harmonics that most affect the current waveform, the PF automatically rises as the current waveform now has its fundamental component as the predominant element. These filters are normally located in the power input line, just before the rectifier circuit, and as with the inductive filter analyzed before, it is constructed with an inductor and a capacitor in parallel and can be complemented with inductive filters in series on the AC side (Fig. 8). Since these filters are tuned to a certain frequency, it is possible to eliminate more than one harmonic component, for which it is only necessary to install a new shunt filter for each frequency. Consequently, the only important design criterion to consider is that each filter is tuned to the correct frequency.

Series resonant filter

It could be considered as a general case of the series filter with resonance tuning. In this type of connection, different LC circuits tuned in series with the power supply are used (Fig. 9) (Ji & Wang, 1998; Prasad et al., 1990). If a single LC block is used, then the resonance is only tuned to a single harmonic frequency, but it is common to see it in multi-tuned structures, i.e., with more than one LC block. The example shown in Fig. 9 contains, in addition to the series filter on the AC side, two resonant series blocks, one tuned to the third harmonic (L_{r3} and C_{r3}) and the other tuned for high frequencies (L_{rh} and C_{rh}).

Output filter

Another passive strategy used to reduce the harmonic content in the input current of a rectifier is the use of a filter in the output stage, to increase the conduction time of the current in each half-cycle of the signal. This strategy

ISSN 1692-8407

Figure 5

Waveforms in the ideal case of the inductive L-filter.

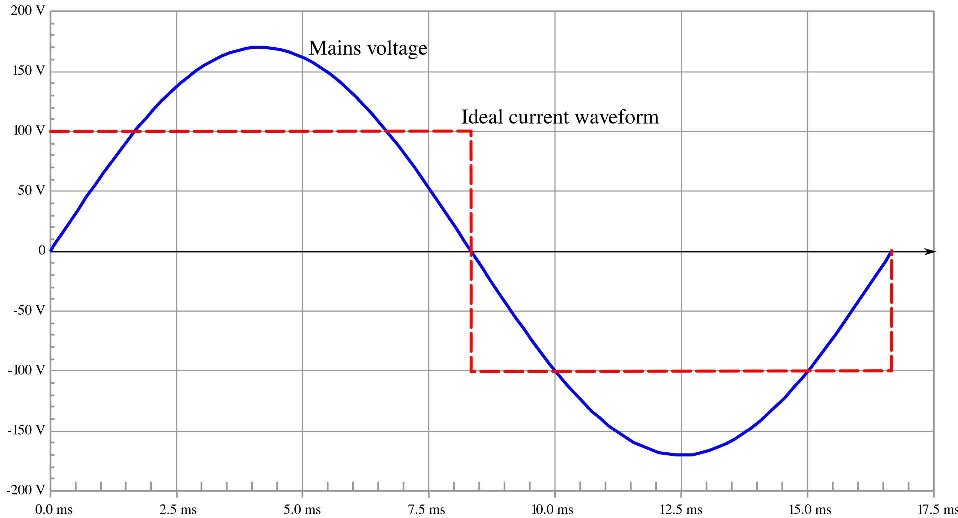

Figure 6

Inductive filter alternative solution.

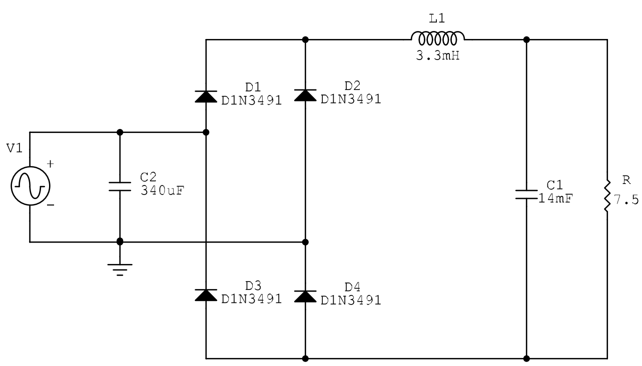

uses an inductor in series after the rectifier circuit that keeps the current flowing to the load for a longer time (Fig. 10). This inductive element is designed to work with the ripple produced in the rectification, i.e., a low frequency equivalent to twice the mains frequency. Moreover, at this point, there is an average DC that the inductor must handle without saturating. This is why these inductors are known as choke and are designed with special cores or magnetic elements with gaps in their magnetic circuits. This choke tends to be large, so to reduce its volume and cost a small capacitor C_f is used in parallel with the bridge rectifier, which completes the output filter (Redl, 1998). It is also usual in this configuration a diode in series with the choke to prevent current flow from the choke to the capacitor when the rectifier voltage is lower than that stored in the output capacitor C_0 (if the capacitor of the filter L is not used, then the diode is not necessary, and all the filtering falls on the choke and the output capacitor C_0).

Active methods

These strategies use some active-controlled elements such as transistors or thyristors to reconstruct the current signal waveform by continuously tracking the behavior of the voltage signal, which serves as a reference. While most cases (which are the ones detailed in this article) use these active elements in the output stage of the rectifier circuit, there are also active rectification schemes in which the controlled active element is part of the rectifier circuit. Since they are beyond the scope of this research, we do not detail them here, but they can be consulted in the related publications (Martínez, 2003).

Boost converter

The Boost converter is the most used power topology in active PF correction circuits. This topology has several features that make it suitable for this type of application, such as presenting a continuous output current (in circuits operating in continuous operation mode at least) thanks to the choke at the output, whose value can be tracked directly in these elements to make current control, which has been shown to ensure the stability of the converter. In addition, it is an easily controlled booster circuit, which allows any voltage value higher than the input voltage to be obtained at

ISSN 1692-8407

Figure 7

Input voltage and current in the inductive filtered circuit.

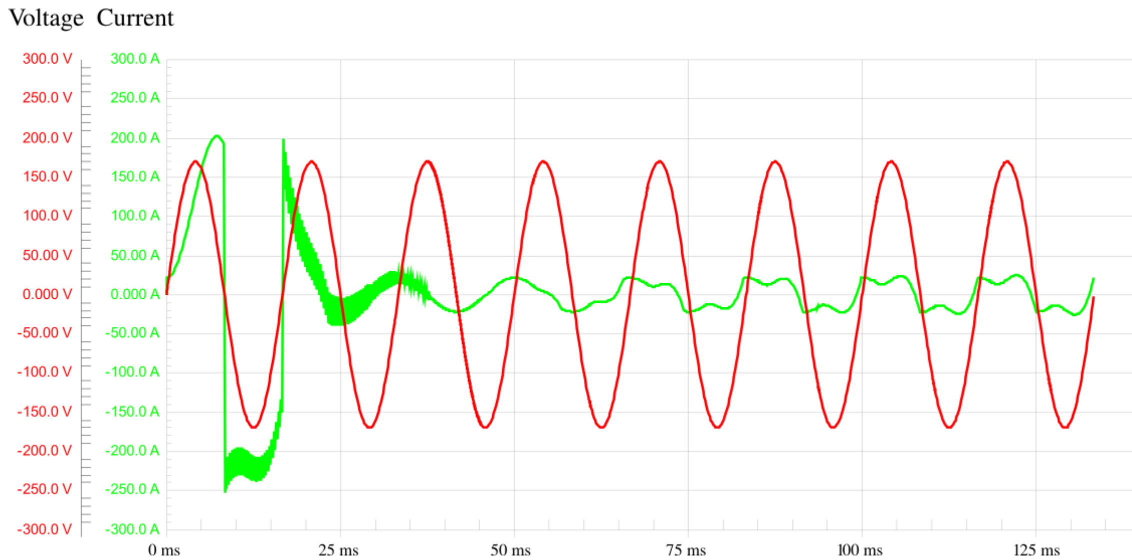

Figure 8

Typical configuration of a parallel resonant filter.

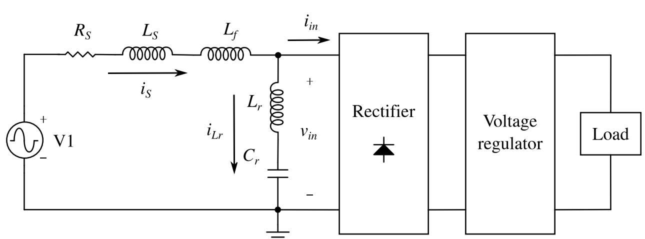

Figure 9

Typical configuration of a series resonant filter.

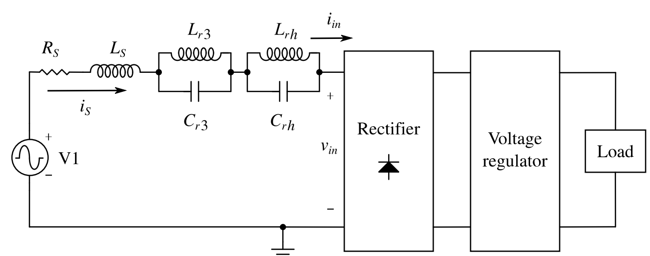

the output. Among the disadvantages, however, is the fact of not having galvanic isolation between input and output, and the restriction of use to low and medium powers.

Like all switched converters, its operating principle is based on the switching of the active switch at a frequency much higher than the mains frequency. When the average duty cycle value is modulated, the average value of the converter input voltage can be controlled. However, if you simultaneously vary this average behavior to follow the instantaneous value of the sinusoidal input voltage signal, then the average current signal drawn by the converter from the mains will also be sinusoidal and in phase with the mains voltage, making the entire converter look like some kind of linear resistance (Fig. 11). The converter is a non-linear circuit, but by operating in this way the network sees it as a linear load, for this reason, these circuits are known as

Figure 10

LC Output filter.

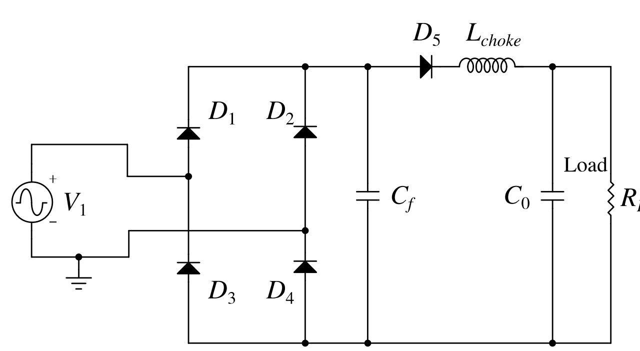

ISSN 1692-8407

resistive emulators. The control algorithm used in these converters can be widely different, from traditional PID to neural systems and sliding controls. The important thing in all cases is that the response of the control unit should be much faster than the switching speed of the circuit, which often requires the use of pre-recorded memories with the simulated scheme for any operating condition (something common in fuzzy control schemes).

Other power converters

In cases where a lower output voltage than the input voltage is required, or some wider voltage regulation characteristic, it is normal that the Boost topology is replaced by others such as the Buck converter, Buck-Boost, SEPIC, or CUK (Dacol et al., 2019; Dixit et al., 2019; Eckstein et al., 2019). The latter topologies have the advantage of allowing galvanic isolation, and even continuous output current, something that is not possible without an additional filter with the Buck converter. The control principle in these converters is usually the same as with the Boost converter, two control loops are used, a voltage loop to regulate the output voltage, and a current loop to ensure stability and reconstruction of the current signal. The control loop is of a higher frequency than the switching frequency, while the voltage loop can be slower, close to the frequency of the power grid.

Hybrid methods

The best performance at the lowest cost is achieved by combining active and passive solutions. This type of strategy is called hybrid and has the advantages of the control schemes of the active strategies, and the corresponding advantages of the active elements, such as a resonant operation that reduces the switching powers, and therefore increase the efficiency of the circuits considerably (Jithin & Cherian, 2018; I. Lee, 2015; I.-O. Lee, 2016).

Conclusion

It is clear the need to reduce the harmonic content in single-phase rectifier circuits, its widespread use in everyday equipment makes the injection of harmonics to the network becomes every day a more critical problem. In this article a categorization of the existing methods has been made, however, the variety and quantity are so wide that it is impossible to record them all in a document like this. However, the schemes widely known in the scientific community are recorded, as well as their most important characteristics. This classification emphasizes two schemes, the use of passive filters (which were simulated in a real circuit) and the active strategies based on high-frequency switching of a power converter. The combination of these two basic strategies seems to be the path taken by the most recent research.

References

Akther, M. S., Lubna, N., Anika, L. T., Jannat, M. M., & Mubassera, J. Series connected active multipulse rectifiers for harmonics mitigation. In: *2019 international conference on mechatronics, remote sensing, information systems and industrial information technologies (ICMRSISIIT)*. 2019, 168543. https : / / doi . org / 10 . 1109 / ICMRSISIIT46373.2020.9405921.

Dacol, R. P., Heerdt, J. A., & Waltrich, G. Non-isolated high current battery charger with PFC semi-bridgeless rectifier. In: *2019 IEEE 15th brazilian power electronics conference and 5th IEEE southern power electronics conference (COBEP/SPEC)*. 2019, 1–6. https://doi.org/10.1109/COBEP/SPEC44138.2019.9065719.

de Souza, A. F., Ribeiro, E. R., Vicente, E. M., & Tofoli, F. L. (2019). Experimental evaluation of active power factor correction techniques in a single-phase AC-DC boost converter. *International Journal of Circuit Theory and Applications*, *47*(9), 1529–1553. https://doi.org/10.1002/cta.2664

Dixit, A., Pande, K., Rathore, A. K., Singh, R. K., & Mishra, S. K. Design & development of on-board DC fast chargers for e-rickshaw. In: *2019 IEEE transportation electrification conference (ITEC-india)*. 2019, 1–6. https://doi.org/10.1109/ITEC-India48457.2019.ITECIndia2019-40.

Eckstein, R. H., Lazzarin, T. B., & Waltrich, G. Two-stage SEPIC-buck topology for neighborhood electric vehicle charger. In: *2019 IEEE 15th brazilian power electronics conference and 5th IEEE southern power electronics conference (COBEP/SPEC)*. 2019, 1–6. https://doi.org/10.1109/COBEP/SPEC44138.2019.9065423.

Jauch, F., & Biela, J. (2016). Combined phase shift and frequency modulation of a dual active bridge AC-DC converter with PFC. *IEEE Transactions on Power Electronics*, *31*(12), 1–1. https://doi.org/10.1109/TPEL.2016.2515850

Ji, Y., & Wang, F. (1998). Single-phase diode rectifier with novel passive filter. *IEE Proceedings - Circuits, Devices and Systems*, *145*(4), 254. https://doi.org/10.1049/ip-cds:19982034

Jithin, K., & Cherian, E. Hybrid DC-DC converter for EV battery charger with bridgeless powerfactor correction. In: *2018 4th international conference for convergence in technology (i2ct)*. 2018, 1–6. https://doi.org/10.1109/I2CT42659.2018.9057864.

ISSN 1692-8407

Figure 11

Boost converter current shaping circuit.

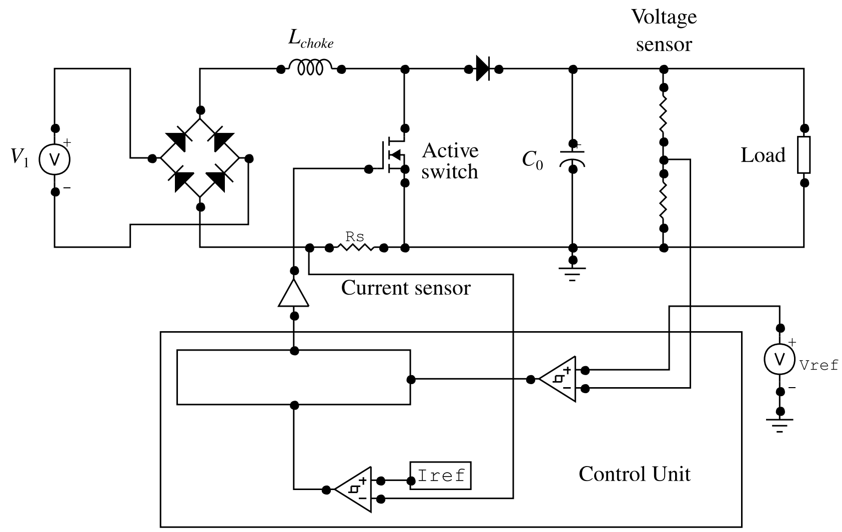

Kazem, H. Input current waveshaping methods applied to single-phase rectifier. In: *Proceeding of international conference on electrical machines and systems*. 2007, 54–57.

Lee, I. (2015). A hybrid pwm-resonant dc-dc converter for electric vehicle battery charger applications. *Journal of Power Electronics*, *15*(5), 1158–1167. https://doi.org/10.6113/JPE.2015.15.5.1158

Lee, I.-O. (2016). Hybrid DC–DC converter with phase-shift or frequency modulation for NEV battery charger. *IEEE Transactions on Industrial Electronics*, *63*(2), 884–893. https://doi.org/10.1109/TIE.2015.2477345

Liu, Z., Lee, F., Li, Q., & Yang, Y. (2016). Design of GaN-based MHz totem-pole PFC rectifier. *IEEE Journal of Emerging and Selected Topics in Power Electronics*, *4*(3), 799–807. https://doi.org/10.1109/JESTPE.2016.2571299

Martínez, F. (2001). El fenómeno de distorsión armónica en redes eléctricas. *Tecnura*, *5*(9), 46–54.

Martínez, F. (2003). Técnicas de conversión ac/dc en sistemas monofásicos con factor de potencia unitario. *Tecnura*, *6*(12), 31–41.

Martínez, F. (2009a). Evaluating neural control with optimal architecture for dc/dc converter. *Ingeniería e Investigación*, *29*(3), 134–138.

Martínez, F. (2009b). Increase the boost converter performance using genetic algorithms. *The Online Journal on Electronics and Electrical Engineering*, *2*(1), 179–182.

Martínez, F., & Gómez, D. (2004). Corrección activa del factor de potencia en cargas no lineales. *Tecnura*, *7*(14), 40–47.

Martínez, F., & Gómez, D. Fuzzy logic controller for boost converter with active power factor correction. In: *7th international conference on power electronics (icpe 2007)*. *7*. 2007, 936–940.

Martínez, F., & Gómez, D. (2012). Optimization of a neural architecture for the direct control of a boost converter. *Tecnura*, *16*(32), 41–49.

Martínez, F., Hernández, C., & Jacinto, E. (2013). Rectificador de alto desempeño para aplicaciones de media potencia en equipos con alimentación universal. *Tekhnê*, *10*(1), 19–27.

Martínez, F., & Jacinto, E. (2013). Power factor corrector with pid loop fit by genetic algorithm. *Tecnura*, *17*(2), 10–17.

Martínez, F., Martínez, F., & Jacinto, E. Strategy for the selection of reactive power in an industrial installation using k-means clustering. In: *International conference on data mining and big data*. 2019, 146–153.

Monteiro, V., Tashakor, N., Tanta, M., Afonso, J. A., Martins, J. S., & Afonso, J. L. A proposed single-phase five-level PFC rectifier for smart grid applications: An experimental evaluation. In: *IECON 2019 - 45th annual conference of the IEEE industrial electronics society*. 2019, 1–6. https://doi.org/10.1109/IECON.2019.8926971.

ISSN 1692-8407

Nagel, L. W., & McAndrew, C. C. Why SPICE is just as good and just as bad for IC design as it was 40 years ago. In: *2018 48th european solid-state device research conference (ESSDERC)*. 2018, 1–6. https://doi.org/10.1109/ESSDERC.2018.8486875.

Ochoa, Y., Rodríguez, J., & Martínez, F. (2017). Low cost regulation and load control system for low power wind turbine. *Contemporary Engineering Sciences*, *10*(28), 1391–1399.

Pahlevani, M., Pan, S., Eren, S., Bakhshai, A., & Jain, P. (2014). An adaptive nonlinear current observer for boost PFC AC/DC converters. *IEEE Transactions on Industrial Electronics*, *61*(12), 6720–6729. https://doi.org/10.1109/TIE.2014.2316216

Prasad, A., Ziogas, P., & Manias, S. (1990). A novel passive waveshaping method for single-phase diode rectifiers. *IEEE Transactions on Industrial Electronics*, *37*(6), 521–530. https://doi.org/10.1109/41.103457

Redl, R. An economical single-phase passive power-factor-corrected rectifier: Topology, operation, extensions, and design for compliance. In: *APEC '98 thirteenth annual applied power electronics conference and exposition*. IEEE, 1998, 1–6. https://doi.org/10.1109/APEC.1998.647729.

Riaño, J., Ladino, C., & Martínez, F. (2012). Implementación de la transformada fft sobre una fpga orientada a su aplicación en convertidores electrónicos de potencia. *Tekhnê*, *9*, 21–32.

Sellers, A. J., Hontz, M. R., Khanna, R., Lemmon, A. N., & Shahabi, A. An automated SPICE modeling procedure utilizing static and dynamic characterization of power FETs. In: *2018 IEEE applied power electronics conference and exposition (APEC)*. 2018, 1–6. https://doi.org/10.1109/APEC.2018.8341019.

Vásquez, M., & Martínez, F. (2011). Control difuso-deslizante para convertidor dc/dc. *Tekhnê*, *8*, 31–40.